Cleaner Engineering and Technology 2 (2021) 100048

Contents lists available at ScienceDirect

Cleaner Engineering and Technology

journal homepage: www.journals.elsevier.com/cleaner-engineering-and-technology

An application of seasonal borehole thermal energy system in Finland

Hafiz Haq [a,*], Petri Välisuo [a], Lucio Mesquita [b], Lauri Kumpulainen [a], Seppo Niemi [a]

[a] School of Technology and Innovation, University of Vaasa, Vaasa, Finland
[b] Natural Resources Canada, CanmetENERGY, Ottawa, Ontario, Canada

ARTICLE INFO

Keywords:
borehole Thermal energy storage
4G district heating system
3D model of ground heat storage
Artificial neural network model
Low temperature heating network

ABSTRACT

Borehole thermal energy system is an important component of the future low temperature heating networks. Applications of such systems are available around the world presenting various configurations. However, the mobility of the system from solar assisted to industrial heat has not yet evaluated. A 3D model of borehole thermal energy system created similar to Drake landing solar community project configuration. This model is validated with experimental measurements. The accuracy of the model estimated at 95%. Experimental measurements further utilized to create an artificial neural network model to predict modes of operation (charging/discharging). The accuracy of the model calculated at 97%. This study presents a possible application of storing excess heat from combined heat and power plants in Sodankylä, Finland. The municipality of Sodankylä is planning construction of new combined heat and power plants. These plants systematically shutdown during summer season leaving 1.53 MW of excess heat. The heat surplus can be stored in a heat storage. Simulations reveal that the model has storage capacity between 250 kW and 285 kW. In addition, there is a potential of five borehole thermal energy storage to store the entire excess heat. The novelty of the study is to test the mobility of borehole thermal energy system from solar assisted storage to industrial excess heat storage. The model used in a standardized manner considering the conventional combined heat and power plants supply temperature for working configuration of heat storage.

1. Introduction

Europe's strategy on district heating and cooling (DHC) encourages to decarbonisation of buildings, energy efficiency management, automation and control, and reuse industrial waste heat (EU strategy, 2016). In 2012, DHC supplied by renewable energy sources amounts to 14% in Europe and 45% in Finland (EU analysis, 2020). The use of fossil fuels in DHC expected to replace by wind power, heat pump and heat storage (Smart energy transition, 2018). Adaptation of renewable energy sources increased recently with industrial heat pumps and deep borehole heat in Finland. This transformation towards the future of district heat production brings challenges in energy efficiency of buildings, integration of solar assisted heat production, and energy production in cold climate (Paiho and Reda, 2016). Integrating heat pumps in decentralized heat production widely accepted in Finnish climate (Laitinen et al., 2014). The recent global commitment to DHC and recognition of carbon dioxide emission reduction identified as moderate (Werner, 2017). However, Europe is eager to increase energy production with DHC with a clear emphasis on utilising renewable sources and reducing carbon dioxide emissions.

The next conceptual phase of heat production appears to be 4-generation district heating and cooling system (4GDHC) (Lund et al., 2014). This allows the implementation of low temperature thermal grid, integration of smart energy systems, waste heat recycling, and low energy space heating. Low energy DHC is comparatively expensive than the conventional heat production (Kofinger et al., 2016). However, the expectations are positive for low energy DHC network implementation. This requires demand-side management and renovation of pipes in the network (Energistyrelsen, 2011). Refurbishment of buildings and installation of substations recommended in some cases (Brand and Svendsen, 2013). Potential to reduce supply temperature in DHC systems is sufficient. Ostergaard and Svendsen (2017) reported the benefits of reducing the supply temperature to 45 °C on several Danish single-family houses. Supply temperature of DHC system as low as 35 °C in a high heat density region investigated by carefully assessing the return temperature (Yang and Svendsen, 2017). The implementation of ultra-low supply temperature could significantly improve the performance fifth generation DHC systems. This allows heat producers to reduce heat losses and take the opportunity to integrate variety of low-temperature waste heat sources (Rhein et al., 2019). In addition, models of building and DHC,

* Corresponding author.
E-mail address: hafiz.haq@uva.fi (H. Haq).

https://doi.org/10.1016/j.clet.2021.100048
Received 17 July 2020; Received in revised form 30 January 2021; Accepted 30 January 2021

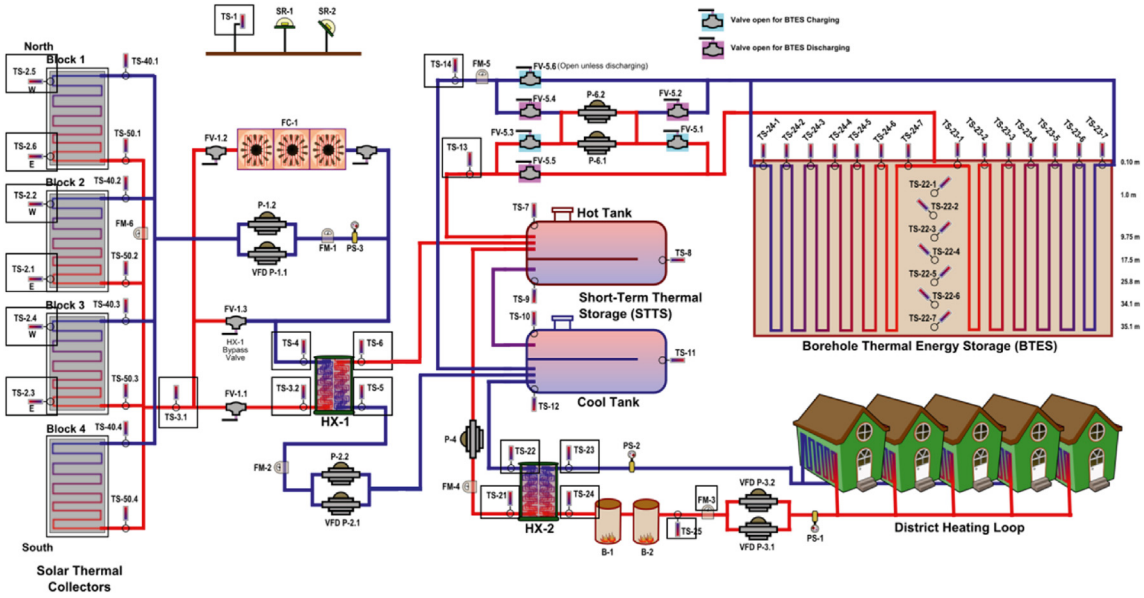

Fig. 1. Schematic diagram of the system. The schematic shows the positions of all the temperature sensors, flow meters, pump and valves. The collected dataset used in the study is marked with green box.

energy transport losses, and indoor climate should be analyse for maximising efficiency (Risberg et al., 2015). An important component of implementing future DHC is Borehole thermal energy system (BTES). A BTES implements either in centralized or decentralized heat production. Installation of BTES also presents challenges such as design of the system, energy management between injection and extraction, and heat losses (Li and Wang, 2014). Design parameters of BTES has significant effect on the performance of heating system along with the temperature of the storage. High storage temperature required for heat distribution in big districts (Nordell, 1994). Location of the BTES needs consideration before installation of the system. Heat losses from BTES vary in different climate. Flynn and Siren (2015) investigated the performance of seasonal BTES in five different locations. Results indicated that insulation and low temperature heating system influence the performance of the storage. The northern countries specially requires optimal design to keep stable performance. A BTES requires heat source to store heat energy, which can either decentralized or centralized application (Nussbicker-Lux et al., 2009). In Europe, heat storage extensively used with biomass boilers and combined heat and power plants (Fisch et al., 1998). The capacity of a BTES design depends on either medium borehole or shallow borehole system. Nilsson and Rohdin (2019) evaluated the performance of large-scale BTES in Emmaboda, Sweden. Results indicated that the quantity of heat source influenced the heat extraction from BTES. Application of medium-scale BTES appears more suitable for DHC system application (Rad et al., 2017). However, performance of a BTES determines by optimal design models. Kandiah and Lightstone (2016) investigated an optimized BTES with a buried tank to save ground space. Results revealed that the presence of a tank did not significantly reduce the performance of BTES. Furthermore, comparative performance between a centralized and decentralized district heating system is of importance. Losses in a decentralized DHC found to be less than the centralized system (Rehman et al., 2018).

There is clear gap in the previous research to propose a standard BTES model that can be use in multiple applications such as solar assisted and waste heat. This study proposes a 3D model of BTES and validates with experimental measurements collected from drake landing solar community (DLSC) project organizer. Eleven years of experimental measurements analysed and key information presented. This data also used to create an artificial neural network model for identifying modes of operation (charging or discharging). The model of BTES employed to store excess heat from combined heat and power (CHP) plants. Charging operations simulated for summer season storing excess heat and discharging operation simulated for rest of the year. Next section presents analysis of DLSC system and artificial neural network model. The following section propose the model of BTES. Results projected in section four. Section five shows applications of BTES and the study concludes in section six.

2. System description

Drake Landing Solar Community (DLSC) project analysed in this study to model BTES and store excess heat from CHP plants. The schematic diagram of the project presented in Fig. 1. Main components of the system consists of solar thermal collectors (Sibbit et al., 2012), short term thermal storage (STTS), borehole thermal energy system (BTES) (Sibbit et al., 2007), heat exchangers (HX), boilers (B), cooling fans (FC), and district heating loop (Renaldi and Friedrich, 2019). There are several temperature sensors (TS), flow meters (FM), pumps (P), and flow valves (FV) to control the mode of operation. The system supplies heat to the district as well as stores heat in BTES depending on heat demand (Sibbit et al., 2015). The cooling fans installed to mitigate the excess heat from solar thermal collectors. Hot and cold tanks connected to the supply and return distribution lines (Sibbit et al., 2011). Boilers function as compensation if supply temperature is lower than the demand of the loop. The system further elaborated in (Mesquita et al., 2017).

2.1. Borehole thermal energy system

The focus of the study is to construct a 3D model of the BTES similar to DLSC project. Therefore, information related to the BTES extracted from the schematic shown in Fig. 1. Sensor measurements recorded every 10 min. Flow valve (FV) controls the movement of carrier fluid in and out of the BTES. Flow meter (FM) recorded volumetric flow rate of the carrier fluid. Inlet (TS-13) and outlet (TS-14) temperature sensors recorded the temperatures to and from the BTES. The data consists of eleven years of sensor measurements. Dataset consists over half a million samples recorded over eleven years of operation every 10 min. This information helps evaluating the optimal design constraints of a centralized or decentralized heat production system. The annual mean air temperature of the region measured at 5 °C with a standard deviation of 11.6 °C. The coldest annual air temperature recorded at −34 °C. The average BTES

Table 1
Parameters used in the artificial neural network model.

Parameter	Value
Model type	Classification-learning method
Number of hidden layer	1
Number of nodes	18
Activation function of hidden layer	Relu
Number of output layer	2
Activation function of output layer	Softmax
Optimizer for compilation	Adam
Loss function	Categorical-crossentropy
Validation split	20%
Number of epochs	10
Input	(TS-7–TS-14), (TS-22-1-TS-22-7), (TS-23-1-TS-23-7), (TS-24-1-TS-24-7), (FM-4-FM-5), (FV-5.1-FV-5.6)
Output	BTES_CHARGING, BTES_DISCHARGING

temperature measured at 38 °C. The average temperature of the hot (TS-8) and cold (TS-11) tank recorded at 55 °C and 47 °C. The minimum, mean and maximum temperature of inlet carrier fluid (TS-13) measured at 0 °C, 55 °C and 89 °C. The mean and maximum volumetric flow rate (FM-5) of the carrier fluid recorded at 1.6 l/s and 4.5 l/s. The percentage of charging and discharging operation of BTES during eleven years estimated at 43% and 20% of the time. The boiler 1 (B-1) and boiler 2 (B-2) used around 1.13% and 5.61% of the time.

2.2. Mode of operation

The dataset contains information on mode of operation (charging/discharging). The mode of operation represents status signal recorded with "BTESCHARGING" and "BTESDISCHARGING". During charging mode, valves FV-5.1, FV-5.3, and FV-5.6 switched on. Discharging mode, however, switched on valves FV-5.2, FV-5.4, and FV-5.5. The collected dataset indicates five months (May–October) of charging operation performed every year. This means when temperature of STTS (TS-8) is greater than twice the required temperature of the consumer, the charging switches on. Charging operation discontinues if the difference between inlet (TS-13) and outlet (TS-14) temperature is less than 5 °C. However, there are fluctuations in the charging operation. Discharging switches on when temperature of STTS (TS-8) is smaller than inlet (TS-13) temperature.

Table 2
Parameters used in Sodankylä model.

Name	Symbol	Value
Thermal conductivity of the ground	k_g	1.07 (W/m·K)
Density of the ground	ρ	1520 (kg/m^3)
Specific heat capacity of the ground	C_p	1014 (J/kg·K)
Inner diameter of heat exchanger	d_i	25 (mm)
Inner diameter of inlet and outlet	d_{iio}	65 (mm)
Thickness of pipes	d_t	1.5 (mm)
Depth of heat exchanger	D	35 (m)
borehole to borehole distance	D_b	2.25 (m)

3. Methodology

This section presents models of artificial neural network and BTES. Machine learning implemented to Train artificial neural network models (Datacamp, 2020). Artificial neural network model represents the mode of operation (charging/discharging). Mathematical modelling of BTES reveals numerous characteristics and applicability (Hellstrom, 1991; Eskilson, 1987). These models improved to understand the thermal properties of BTES applications (Al-Khoury et al., 2005; Al-Khoury and Bonnier, 2006). FEFLOW is one example used to model and simulate the performance (Diersch et al., 2011). Recent study reveal the influence of groundwater and air temperature (Nguyen et al., 2017). Uncertainty in the ground modelled using the experimental data to create multilayers of the ground, studying the thermal properties and the possibilities to expand the existing project (Tordrup et al., 2017). 3D model of BTES created to study the performance in short-term (Haq and Hiltunen, 2019).

3.1. Artificial neural network

The mode of operation (charging/discharging) of BTES modelled with artificial neural network. This model uses input and output information from the dataset to mimic charging and discharging modes of BTES. Input data consists of temperature, volumetric flow rate, and flow valve measurements. Output data includes status signals for charging and discharging modes. During the charging operation, the dataset indicates "BTESCHARGING = 1" and "BTESDISCHARGING = 0". The discharging operation indicates "BTESCHARGING = 0" and "BTESDISCHARGING = 1". Classification-learning method used to train the output variables. Parameters of the model shown in Table 1.

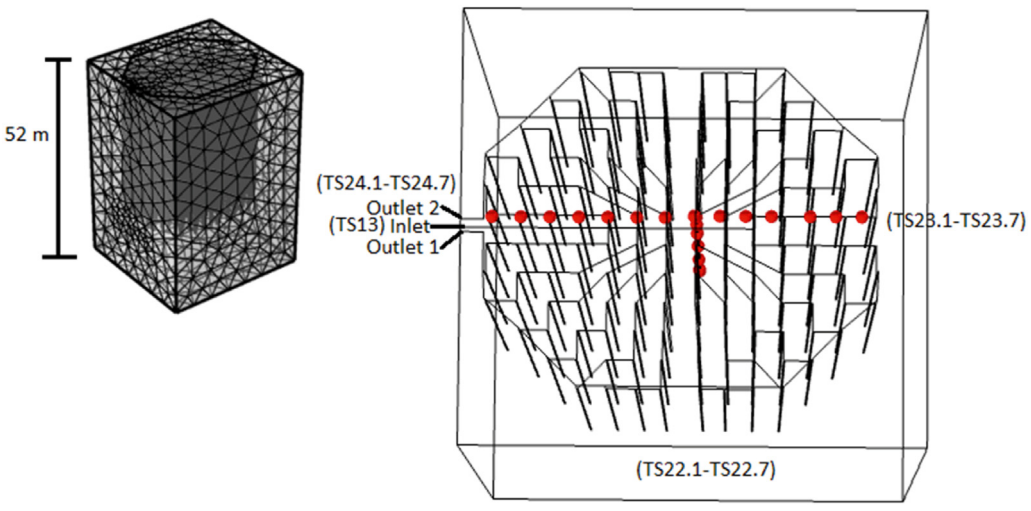

Fig. 2. 3D model of the Borehole Thermal Energy Storage (BTES). Red-dots show the position of the sensors in the system. TS22.1-TS22.7 are the core temperature measurements. TS23.1-TS23.7 and TS24.1-TS24.7 are the ground temperature measurements.

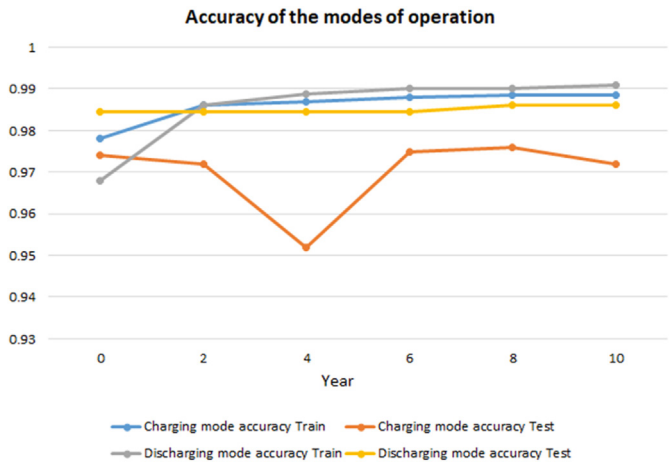

Fig. 3. Accuracy of artificial neural network model for modes of operation.

3.2. Borehole thermal energy system

BTES model implemented in Comsol multiphysics. The hexagonal shaped BTES consists of 144 boreholes heat exchanger pipes shown in Fig. 2. There are six heat exchanger pipes connected in series between inlet and outlet making up 24 strings in total. Each heat exchanger pipe has a depth of 35 m and 2.25 m distance between them. The dimensions of the ground are 36 × 34 × 52 m. The material properties presented in Table 2. The temperature sensors represented as (TS). The position of these sensors depicted with red dots. The core temperatures illustrated as (TS22.1 to TS22.7), ground temperature from centre to right, shown as (TS23.1 to TS23.7), ground temperature from centre to left, presented as (TS24.1 to TS24.7) and inlet temperature represented as (TS13). The boundary conditions consist of inlet temperature (TS13), volumetric flow rate and the initial temperature of the ground.

There are two modules used to simulate the model namely, Heat transfer in Solids and Non-isothermal pipe flow. Heat transfer module is required to compute heat transfer in the ground caused by the heat exchanger pipes. Non-isothermal pipe flow module computes heat transfer caused by the fluid flow in the heat exchanger pipes. Heat transfer in the ground expressed as:

$$\rho C_p \frac{\partial T}{\partial t} + \nabla . q = Q \tag{1}$$

$$q = -k\nabla T \tag{2}$$

Where, ρ (kg/m^3) is density, C_p (J/kg·K) is specific heat capacity, T (^{0}C) is temperature, t (s) is time duration, q (W/m^2) is heat flux, k (W/m·K) is thermal conductivity of the ground and Q (W/m^3) is volumetric heat source in the region. Heat transfer in pipe stated as:

$$\rho A C_p u.\nabla T = \nabla . Ak\nabla T + f_D \frac{\rho A}{2d_h}|u|^3 + Q_{wall} \tag{3}$$

$$Q_{wall} = hZ(T_{ext} - T) \tag{4}$$

Where, u (m/s) is velocity, d_h (m) is hydraulic diameter, f_D is dimensionless Darcy friction factor, and A (m^2) is cross sectional area of the pipe. Where, Q_{wall} (W/m) is external heat transfer and Z (m) is wetted parimeter. A tetrahedral mesh created which consists of 119613 nodes and 60402 edge elements. Comsol software allows adding multiple physics interfaces on the geometry. In this case, Heat transfer in solids and Non-isothermal pipe flow interfaces used in the simulations, which produces output similar to conjugate heat transfer as oppose to computational fluid dynamics (CFD). The model should be validated with experimental measurements. Percentage error is calculated between experimental measurements and simulated calculations (TS23 and TS24). The percentage error expressed as:

$$Error\ (\%) = \frac{|T_{exp} - T_{sim}|}{T_{exp}} \times 100 \tag{5}$$

Where, T_{exp} (^{0}C) is experimental temperature and T_{sim} (^{0}C) is simulated temperature.

4. Results

This section presents results for both artificial neural network and BTES models. The accuracy of BTES charging and discharging modes estimated. Simulation of charging and discharging operation presented in the following section.

4.1. Accuracy of artificial neural network model

The accuracy of the models plotted in Fig. 3. The models predict the signal of charging and discharging operation and have higher accuracy on Train dataset compare to Test dataset. The Train dataset consists of all inputs and outputs parameters, while the Test dataset consists of unknown input parameters. The parameters shown in Table 1. Artificial neural network model trained with Train dataset where it learns the possible output. Test dataset then used to forecast the output with trained model. There is a 20% validation split, which means 20% of the dataset

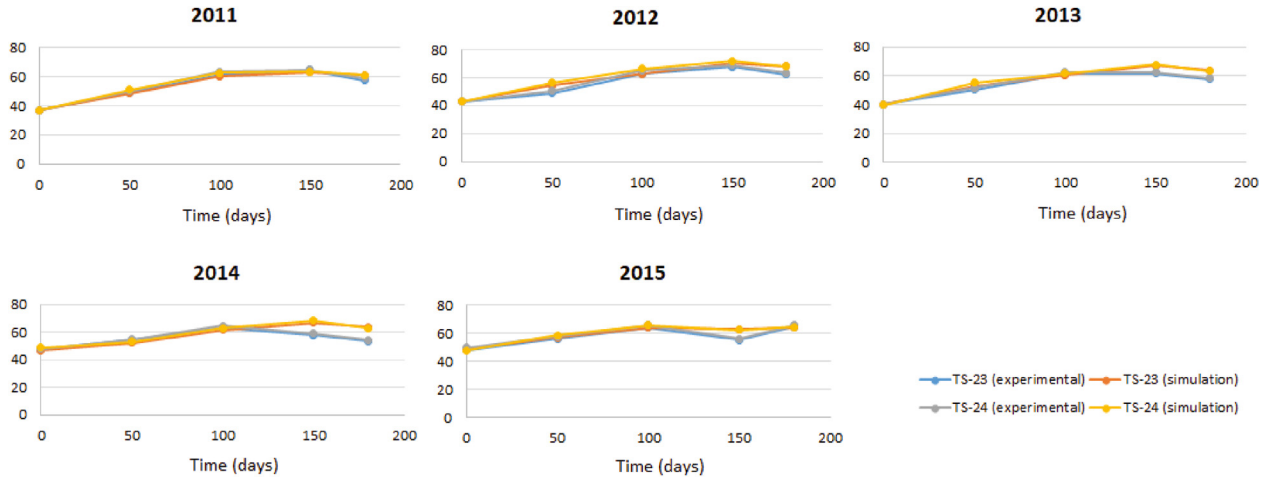

Fig. 4. Average daily surface temperature.

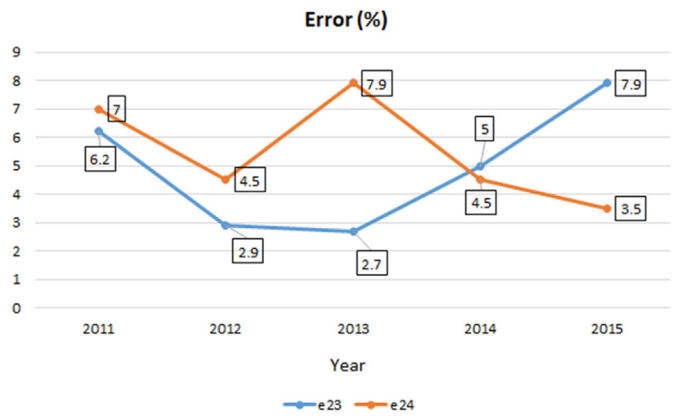

Fig. 5. Percentage error calculation between experimental measurements and simulation results.

separated for validation. The accuracy of the model elaborated as how well the model performs between known inputs and unknown inputs. Charging and discharging operations validated so that it can be used in other similar projects. Both charging and discharging models have an average accuracy over 95%.

4.2. Validating model of borehole thermal energy system

Five simulations conducted to validate the model for each year of charging operation. The collected dataset indicates six months (May–October) of charging operation performed every year. Experimental measurements are the surface temperature of the BTES. Average surface temperatures are always greater than zero (^{0}C) due to the charging strategy. In addition, charging operation starts if the reference temperature is stable. Fig. 4 shows the average daily surface temperature. The system description indicated that (TS22) was faulty. Therefore, TS-23 and TS-24 compared between simulation results and experimental measurements. TS is the temperature sensor measurements referring to the surface temperature of the BTES. There are six months of charging operation simulated during 2011–2015. The data indicates temperature measurement over 40 °C at the beginning of the charging operation and surface temperature rose over 60 °C by the end.

Fig. 5 presents percentage error calculation of charging operation during 2011–2015. The estimation conducted by considering average surface temperature measurements (TS-23 and TS-24). Errors (e23 and e24) represent percentage error between experimental measurement and simulation results. The minimum and maximum errors estimated at 2.54% and 7.8%. The average error between simulated and collected data calculated under 5%.

4.3. Limitations of the model

The model consists of 119613 plus 60402 number of degrees of freedom. High number of degrees of freedom have high latency. Computation of such complex model requires a lot of time to solve the parameters. The model was simplified by reducing the air temperature parameter. The insulation layer at the top and the soil layer were also not considered in the simulation. The input parameter (TS13) was converted into average daily temperature. The simulation was conducted in daily time steps, which reduces the time duration to solve the model compared to hourly simulation. Constant average volumetric flow rate was used instead of variable flow rate. The model was validated for only five months of charging operation instead of the whole year operation. Discharging operation mode could not be validated due to high fluctuation of heat demand during the entire year.

5. Application of borehole thermal energy system in Finland

The municipality of Sodankylä, Finland planned to construct six small-scale CHP plants in order to reduce greenhouse gas emissions and support the local economy of the region. The plants are supposed to produce 4.3 MW of heat energy and contribute to the existing district heat production. These plants are wood-based replacing the use of peat energy source, eliminating the final significant fossil fuel use in the district heat production. The heat demand in the region during summer is significantly less than the winter. The preliminary study of the heat production and consumption indicates a surplus of heat production from June until August. The amount of heat surplus is high enough to investigate the opportunity of constructing heat storage system. The long-term benefit of heat storage construction outweighs the required initial investment. Earlier research reveals the contribution of BTES to utilize industrial heat (Guo et al., 2017; Xu et al., 2018). The stored heat energy

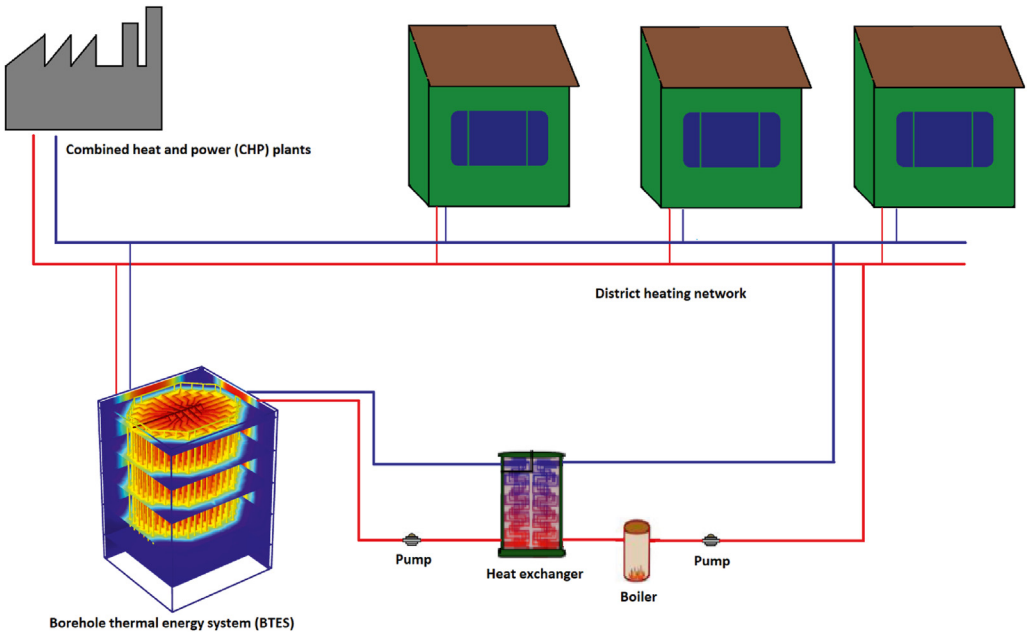

Fig. 6. Application of the proposed BTES. The excess heat from the CHP plants during summer time stored in the BTES and connected with the distribution network.

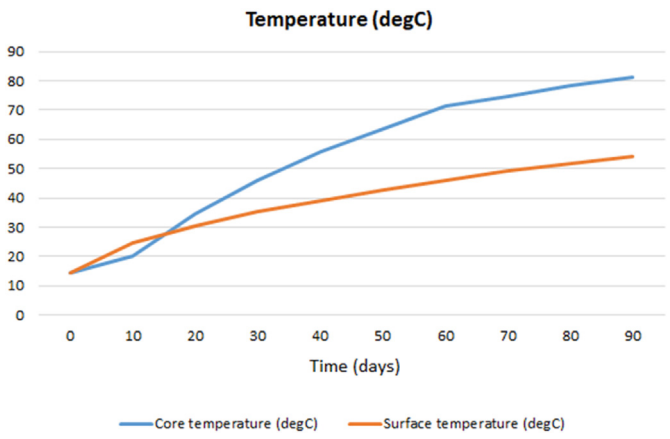

Fig. 7. Core and surface temperature of the BTES during charging operation.

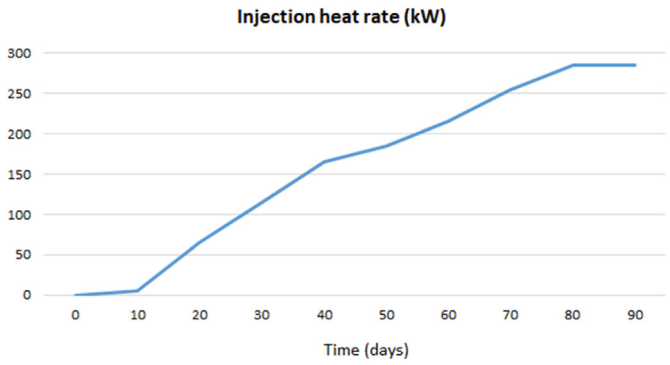

Fig. 8. Heat rate of charging operation.

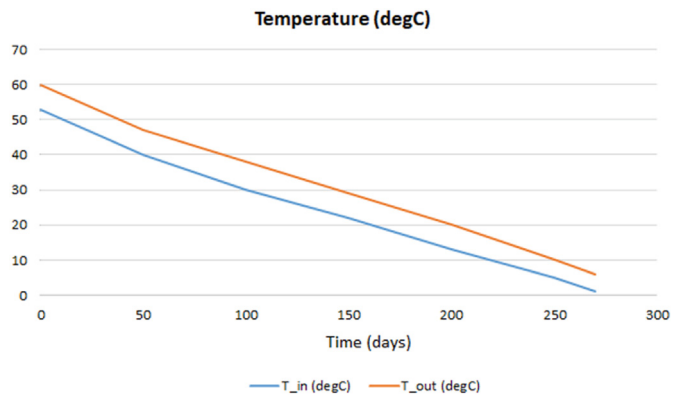

Fig. 9. Inlet and outlet temperature during discharging operation.

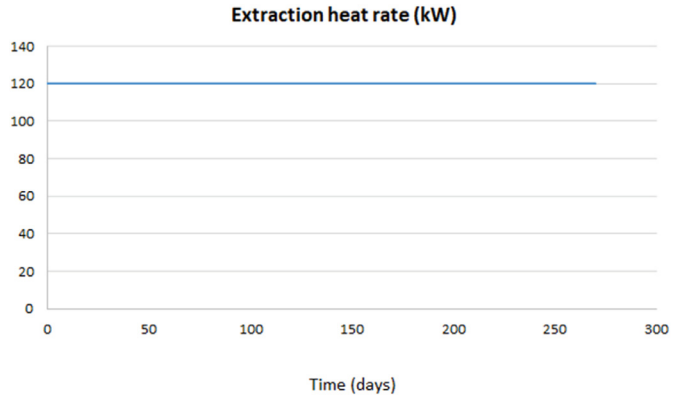

Fig. 10. Heat rate during discharging operation.

contributes to the distribution network during the peak heat demand. The BTES can also be utilized in 4G decentralized district heating systems where the supply temperature is low. The efficiency of BTES reaches 90% in low supply temperature grid after a few years of charging (Guo et al., 2020). The benefits of using BTES in a low temperature small-scale district is significantly higher than a conventional district heating network.

5.1. *Investigating the possibility of borehole thermal energy system installation*

This section proposes an application of BTES with planned CHP plants. According to the preliminary analysis of the project, summer season (June–August) is reserved for service and maintenance. Data analysis of supply and demand of heat energy during summer season indicates a 1.53 MW surplus. This surplus heat energy can be stored in a BTES. Fig. 6 illustrates a possible BTES installation with CHP plants. The CHP plants delivers heat energy to the distribution network. In addition, the supply line can be extended to connect a BTES, which stores excess heat from the CHP plants. The BTES can discharge to the same supply line if needed or it can extend to other distribution network for new construction in the region. Next section simulates charging operation with excess heat. This evaluates the capacity of the BTES and required number of BTES to utilize 1.53 MW surplus heat energy during summer season.

5.2. *Charging borehole thermal energy storage with excess heat*

Initial temperature of the ground assumed to be 6 °C, carrier fluid has an average flowrate of 2 l/s, and constant supply temperature of 90 °C applied to the model. The simulation conducted for 90 days representing the summer season to deliver the available excess heat. One of the restrictions of using BTES is that it takes few years of charging operation to reach a desired temperature before it can be used for discharging operation. The simulation indicated that constant supply temperature from the district heating network insures the core temperature rise of 80 °C shown in Fig. 7. Core temperature (TS22.1-TS22.7) illustrated in Fig. 2. Surface temperature (TS23.1-TS23.7 and TS24.1-TS24.7) estimated at 50 °C at the end of the charging operation.

The energy stored calculated at 0.28 MW at the end of charging operation. Fig. 8 shows the heat rate of charging operation during summer season. The simulation reveals that there is a potential of five BTES of similar dimensions in order to utilize the total amount of excess heat energy from the CHP plants. If the BTES has an efficiency of 40% as estimated in the literature, it means that 86 kW of heat energy is readily available for distribution from each BTES.

5.3. *Discharging borehole thermal energy system*

Discharging operation investigated for short-term operation of the system. Simulation conducted with a constant heat rate of 60 kW. The initial temperature of the BTES considered to be 60 °C, which is the estimated temperature rise at the end of the charging period and suitable for discharging operation rest of the year. Inlet and outlet temperature evaluated with respect to the heat transfer between the heat exchanger pipes and the ground. The volumetric flow rate of the carrier fluid assumed at 2 l/s. The heat capacity of discharging operation is constant for the entire discharging period. The simulation period assumed at 270 days. Fig. 9 shows the inlet and outlet temperature during the discharging operation. The inlet and outlet temperature at the beginning of the simulation estimated at 50 °C and 60 °C respectively. The temperature dropped down to 1 °C and 6 °C at the end of operation.

The temperature gradually decreases over time with a constant heat extraction rate. At the end of the discharging operation, the average

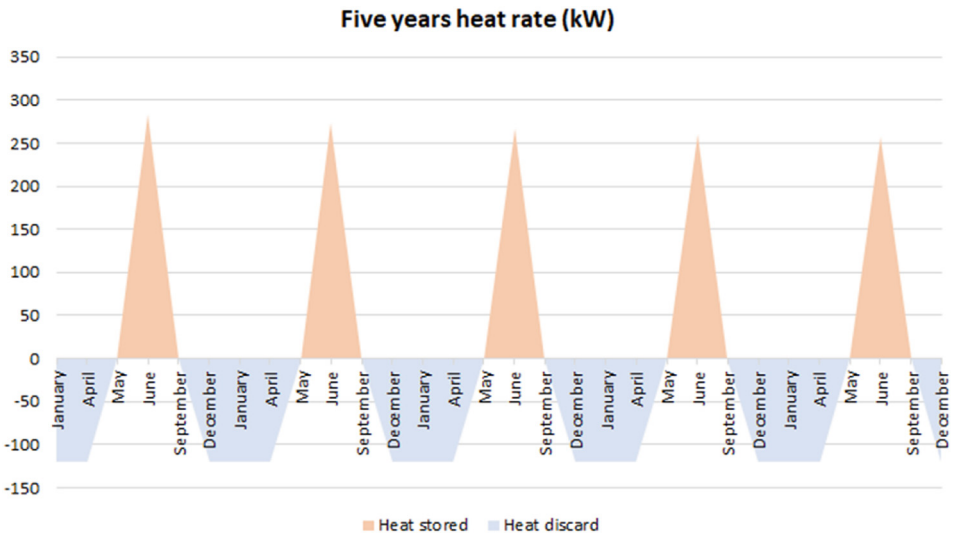

Fig. 11. Heat rate during five years of operation. Charging operation conducted during June–August while discharging took place during September–May.

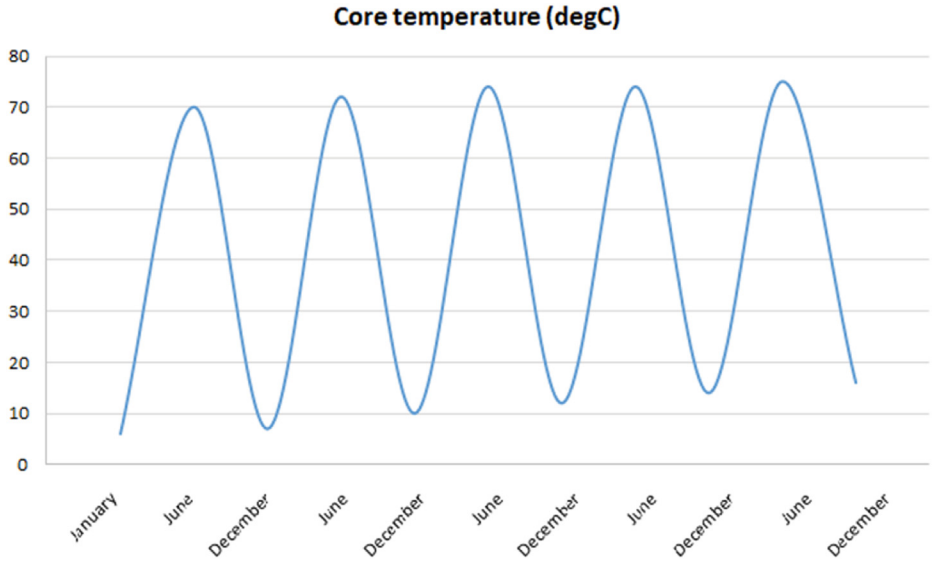

Fig. 12. Average core temperature of the BTES during five years operation.

temperature core estimated at 10 °C. The discharged heat rate is constant at 120 kW illustrated in Fig. 10. In practical scenario, the rate of heat extraction varies with time. If the heat rate of extraction is less than the assumed estimate, the temperature of the BTES will result higher than the calculation. Similarly, if the heat rate of extraction is higher than the assumed estimate, the temperature of the BTES will result lower than the calculation. The point of consideration is to acquire a balance between charging and discharging operation. So that, the BTES can be used for a long period. Another point of consideration is that the temperature of the BTES at the end of the charging operation should not be very high because higher temperature will significantly intensify the heat loss from the BTES. The temperature of the BTES at the end of the discharging operation should not be very low because the lower the temperature of the ground, the longer time it will take to charge at the optimal temperature at the end of the charging season.

5.4. Five years operation of heat storage

In order to evaluate the short-term feasibility of BTES with the proposed mode of operation, the heat injection and extraction forecast in Fig. 11. The heat extraction during the five years operation kept constant which represent the maximum amount of heat extracted for the proposed model. On the other hand, the heat injection during five years operation decreases with time, which represents the temperature increase in the BTES. The plot also shows the duration of heat injection (June–August) and heat extraction (September–May). The heat extraction can be increased, once the heat injection rate is decreased significantly after number of years of operation. The plot depicts a clear representation of the amount of heat rate injected or extracted.

The core temperature illustrated in Fig. 12. Temperature rose to 70 °C at the end of the charging operation of year one. The temperature dropped down to 10 °C at the end of the discharging operation of year one. After five years of operation, the temperature estimated slightly less than 20 °C. It shows the potential to increase the heat extraction rate to balance the operation. The temperature after four years of operation was estimated to be over 70 °C. It shows that heat loss is significantly high which can be optimized by decreasing the injection heat rate.

5.5. Discussion

Charging and discharging operations revealed adequate information on application of heat storage. The model can be connected to the CHP plants storing the released excess heat. The stored heat estimated 0.28 kW, which does not utilize the entire excess heat released from the plants. Additional five BTES is recommended with similar configuration to store surplus heat. These heat storages is beneficial investment because stored heat can be used during winter season to the existing supply network. The heat storage can also be used to deliver heat to remote buildings. Another possible application is a centralized 4G low temperature heating network for new construction. The system can resemble DLSC project with an interchangeable heat source. The DLSC project used fan coils for space heating where the carrier fluid circulated from storage tank to district network at an average temperature of 37 °C. Similar configuration can be taken with floor heating in new residential buildings in the region. The DLSC study concluded that the investment was economically challenging even with the subsidy. The major cost of such system is due to the installation of solar heat collectors. The proposed model combined with excess heat from the CHP plants makes the system economically beneficial.

6. Conclusion

This study focuses on modelling 3D borehole thermal energy system with a possible applications in Sodankylä, Finland. The municipality of Sodankylä is planning the construction of six new CHP plants. Only two of the plants operate during summer season and the rest are shutdown for maintenance, which results in 1.53 MW of excess heat. The excess heat can be stored in a heat storage which is useful during peak winter season. A BTES model created to store excess heat from CHP plants. The configuration parameters of the model were similar to the DLSC project. Experimental dataset of DLSC system was used to validate the BTES model. The accuracy of the model was estimated at 95%. An artificial neural network was created to simulate the modes of operation (charging/discharging). The accuracy was calculated to be 97%. The model could be used in different heat storage applications. The stored excess heat estimated at 0.28 MW during charging operation. Simulations revealed that there is a potential of five BTES installation with similar configuration to utilize the entire excess heat. The capacity of the BTES projected between 285 kW and 250 kW during five years operation.

Ethics approval and consent to participate

Not applicable.

Availability of data and materials

Data that is relevant to the manuscript presented in the text and figures.

Consent for publication

The authors declare full contribution towards the manuscript. The author edited the manuscript and approved of the final manuscript.

Declaration of competing interest

The authors do not intend to compete and declare no competing interests.

Acknowledgement

The author is grateful for the facilities provided by the Faculty of Technology and Innovation, University of Vaasa [Project # 2709000]. The economic estimates and data shared by the Natural Resources Institute of Finland is highly appreciated. The author acknowledges the participation by the Sodankylä Municipality and the Lapland Union. The author is also grateful for the contributions provided by Jukka Lokka from Natural Resource Institute Finland. The authors are very grateful for the data sharing of Drake Landing Solar Community project by Lucio Mesquita from Natural Resources Canada.

References

Al-Khoury, R., Bonnier, P.G., 2006. Efficient finite element formulation for geothermal heating systems. Part II: Transient. Int. J. Numer. Methods Eng. 67, 725–745. https://doi.org/10.1002/nme.1662.

Al-Khoury, R., Bonnier, P.G., Brinkgreve, R.B.J., 2005. Efficient finite element formulation for geothermal heating systems. Part I: steady state. Int. J. Numer. Methods Eng. 63, 988–1013. https://doi.org/10.1002/nme.1313.

An EU, 2016. strategy on Heating and Cooling, Communication from the Commission to the European Parliament, the Council, the European Economic and Social Committee and the Committee of the Region. Brussels.

Brand, Marek, Svendsen, Svend, 2013. Renewable-based low-temperature district heating for existing buildings in various stages of refurbishment. Energy 62, 311–319. https://doi.org/10.1016/j.energy.2013.09.027.

Datacamp, 2020. Careere track. https://learn.datacamp.com/career-tracks/machine-learning-scientist-with-python?version=1. (Accessed 12 November 2020).

Diersch, H.-J.G., Bauer, D., Heidemann, W., Ruhaak a, W., Schatzl, P., 2011. Finite element modeling of borehole heat exchanger systems Part 2. Numerical simulation. Comput. Geosci. 37, 1136–1147. https://doi.org/10.1016/j.cageo.2010.08.002.

Energistyrelsen – EUDP, 2011. CO2-reductions in low-energy buildings and communities by implementation of low-temperature district heating systems. Demonstration cases in EnergyFlexHouse and Boligforeningen Ringgården.

Eskilson, Per, 1987. Thermal Analysis of Heat Extraction Boreholes. Doctoral thesis. University of Lund, Sweden.

EU, 2020. analysis of Heating and Cooling, Mapping and Analyses of the Current and Future (2020 - 2030) Heating/cooling Fuel Deployment (Fossil/renewables), New Energy Technologies, Innovation and Clean Coal. EUROPEAN COMMISSION.

Fisch, M.N., Guigas, M., Dalenback, J.O., 1998. A review of large-scale solar heating systems in europe. Sol. Energy 63, 355–366. https://doi.org/10.1016/S0038-092X(98)00103-0.

Flynn, Ciaran, Siren, Kai, 2015. Influence of location and design on the performance of a solar district heating system equipped with borehole seasonal storage. Renew. Energy 81, 377–388. https://doi.org/10.1016/j.renene.2015.03.036.

Guo, Fang, Yang, Xudong, Xu, Luyi, Torrens, Ignacio, Hensen, Jan, 2017. A central solar-industrial waste heat heating system with large scale borehole thermal storage. Procedia Eng. 205, 1584–1591. https://doi.org/10.1016/j.proeng.2017.10.274.

Guo, Fang, Zhu, Xiaoyue, Zhang, Junyue, Yang, Xudong, 2020. Large-scale living laboratory of seasonal borehole thermal energy storage system for urban district heating. Appl. Energy 264, 1147–1163. https://doi.org/10.1016/j.apenergy.2020.114763.

Hafiz, M.K.U. Haq, Hiltunen, Erkki, 2019. An inquiry of ground heat storage: analysis of experimental measurements and optimization of system's performance. Appl. Therm. Eng. 148, 10–21. https://doi.org/10.1016/j.applthermaleng.2018.11.029.

Hellstrom, Goran, 1991. Ground Heat Storage: Thermal Analysis of Duct Storage System. Doctoral thesis. Lund University, Sweden.

Kandiah, P., Lightstone, M.F., 2016. Modelling of the thermal performance of a borehole field containing a large buried tank. Geothermics 60, 94–104. https://doi.org/10.1016/j.geothermics.2015.12.001.

Kofinger, M., Basciotti, D., Schmidt, R.R., Meissner, E., Doczekal, C., Giovannini, A., 2016. Low temperature district heating in Austria: energetic, ecologic and economic comparison of four case studies. Energy 110, 95–104. https://doi.org/10.1016/j.energy.2015.12.103.

Laitinen, Ari, Tuominen, Pekka, Holopainen, Riikka, Tuomaala, Pekka, Jokisalo, Juha, Eskola, Lari, Sirén, Kai, 2014. Renewable Energy Production of Finnish Heat Pumps, Final Report of the SPF-Project. VTT Technical Research Centre of Finland.

Li, Hongwei, Wang, Stephen Jia, 2014. Challenges in smart low-temperature district heating development, the 6th international conference on applied energy – ICAE2014. Energy Procedia 61, 1472–1475. https://doi.org/10.1016/j.egypro.2014.12.150.

Lund, Henrik, Werner, Sven, Wiltshire, Robin, Svendsen, Svend, Eric Thorsen, Jan, Hvelplund, Frede, Vad Mathiesen, Brian, 2014. 4th Generation District Heating (4GDH) Integrating smart thermal grids into future sustainable energy systems. Energy 68, 1–11. https://doi.org/10.1016/j.energy.2014.02.089.

Mesquita, Lucio, McClenahan, Doug, Thornton, Jeff, Jarrett Carriere, Wong, Bill, 2017. Drake Landing Solar Community: 10 Years of Operation. ISES Solar World Congress. DLSC. https://www.dlsc.ca/reports/swc2017-0033-Mesquita.pdf.

Nguyen, A., Pasquier, P., Marcotte, D., 2017. Borehole thermal energy storage systems under the influence of groundwater flow and time-varying surface temperature. Geothermics 66, 110–118. https://doi.org/10.1016/j.geothermics.2016.11.002.

Nilsson, Emil, Rohdin, Patrik, 2019. Performance evaluation of an industrial borehole thermal energy storage (BTES) project Experiences from the first seven years of operation. Renew. Energy 143, 1022–1034. https://doi.org/10.1016/j.renene.2019.05.020.

Nordell, Bo, 1994. Borehole Heat Store Design Optimization. Doctoral thesis. Lulea University of Technology, Sweden.

Nussbicker-Lux, J., Bauer, D., Marx, R., Heidemann, W., Muller-Steinhagen, H., 2009. Monitoring Results from German Central Solar Heating Plant with Seasonal Thermal Energy Storage. Stockholm, Sweden.

Østergaard, Dorte, Svendsen, Svend, 2017. Space heating with ultra-low-temperature district heating – a case study of four single-family houses from the 1980s. Energy Procedia 116, 226–235. https://doi.org/10.1016/j.egypro.2017.05.070.

Paiho, Satu, Reda, Francesco, 2016. Towards next generation district heating in Finland. Renew. Sustain. Energy Rev. 65, 915–924. https://doi.org/10.1016/j.rser.2016.07.049.

Rad, Farzin M., Fung, Alan S., Rosen, Marc A., 2017. An integrated model for designing a solar community heating system with borehole thermal storage. Energy Sustain. Dev. 36, 6–15. https://doi.org/10.1016/j.esd.2016.10.003.

Renaldi, Renaldi, Friedrich, Daniel, 2019. Techno-economic analysis of a solar district heating system with seasonal thermal storage in the UK. Appl. Energy 236, 388–400. https://doi.org/10.1016/j.apenergy.2018.11.030.

Risberg, Daniel, Vesterlund, Mattias, Westerlund, Lars, Dahl, Jan, 2015. CFD simulation and evaluation of different heating systems installed in low energy building located in sub-arctic climate. Build. Environ. 89, 160–169. https://doi.org/10.1016/j.buildenv.2015.02.024.

Sibbit, B., Onno, T., McClenahan, D., Thornton, J., Brunger, A., Kokko, J., Wong, B., 2007. The Drake Landing Solar Community Project – Early Results. CANMET Energy technology centre, Natural resources Canada, Ottawa, Canada.

Sibbit, B., Mcclenahan, D., Djebbar, R., Paget, K., 2015. Ground Breaking Solar, Case Study Drake Landing Solar Community, High Performing Buildings. ASHRAE.

Smart energy Transition, 2018. Clean District Heating- How Can it Work? Discussion paper, Strategic research. http://smartenergytransition.fi/wp-content/uploads/2018/11/Clean-DHC-discussion-paper_SET_2018.pdf. (Accessed 12 November 2020).

Tordrup, K.W., Poulsen, S.E., Bjørn, H., 2017. An improved method for upscaling borehole thermal energy storage using inverse finite element modelling. Renew. Energy 105, 13–21. https://doi.org/10.1016/j.renene.2016.12.011.

ur Rehman, Hassam, Hirvonen, Janne, Sirén, Kai, 2018. Performance comparison between optimized design of a centralized and semi-decentralized community size solar district heating system. Appl. Energy 229, 1072–1094. https://doi.org/10.1016/j.apenergy.2018.08.064.

von Rhein, Justus, Henze, Gregor P., 2019. Nicholas Long, Yangyang Fu, Development of a topology analysis tool for fifth-generation district heating and cooling networks. Energy Convers. Manag. 196, 705–716. https://doi.org/10.1016/j.enconman.2019.05.066.

Werner, Sven, 2017. International review of district heating and cooling. Energy 137, 617–631. https://doi.org/10.1016/j.energy.2017.04.045.

Xu, Luyi, Ignacio Torrens, J., Guo, Fang, Yang, Xudong, Jan, L.M., 2018. Application of large underground seasonal thermal energy storage in district heating system: a model-based energy performance assessment of a pilot system in Chifeng, China. Appl. Therm. Eng. 137, 319–328. https://doi.org/10.1016/j.applthermaleng.2018.03.047.

Yang, Xiaochen, Svendsen, Svend, 2017. Achieving low return temperature for domestic hot water preparation by ultra-low-temperature district heating, the 15th International Symposium on District Heating and Cooling. Energy Procedia 116, 426–437. https://doi.org/10.1016/j.egypro.2017.05.090.